Addendum III to ATBD

T. Meissner, F. Wentz, D. LeVine and J. Scott

June 04, 2014

This addendum documents change made to the ATBD between V2.0 and V3.0 of the Aquarius L2 salinity retrieval algorithm which was implemented in January, 2014 and that will be released to the public through the JPL PO.DAAC in March, 2014. The code was updated to include all the changes and then the entire data set was re-run.

The algorithm changes that were made concern:

1. Update of the antenna pattern coefficients (APC) to reduce biases in the V-pol and H-pol channels over hot scenes (land) and biases in the 3rd Stokes, which were observed in V2.0.
2. Use of Aquarius derived wind speeds in the surface roughness correction. Two Aquarius wind speed products are produced: HH wind speed using the scatterometer HH-pol and HHH wind speed using the scatterometer HH-pol and the radiometer H-pol.
3. Updated roughness correction using the Aquarius wind speeds, the scatterometer VV-pol and significant wave height (SWH) data.
4. Include H-pol together with V-pol in the salinity retrieval, and updated parameters such as *TB_consistency* to be consistent with this change.
5. An empirical correction to the reflected galactic radiation, which is based on a symmetrization between the ascending and descending swaths. This change reduces the bias between ascending and descending swaths observed in V2.0 and that were traced to the galaxy correction.
6. Inclusion of an adjusted SSS (called SSS_bias_adj) in addition to the standard SSS product. This adjustment is designed to reduce biases observed in the standard SSS product which correlate with SST.
7. A number of quality control flags have been implemented into the L2 product. Their definition and use is specified in [*Meissner, 2014; AQ-014-PS-0006, Le Vine and Meissner, 2014*].
8. A modification to the radiometer drift correction which now uses a 7-day average to compute a bias adjustment to correct for the “wiggles” (residual after the exponential drift correction).

1 Antenna Pattern Coefficients

horn 1			
1	1.0448	-0.0383	+0.0500
2	- 0.0030	1.0786	+0.0300
3	-0.0009	-0.0258	1.0755
horn 2			
1	1.0497	-0.0343	0.0000
2	-0.0006	1.0593	0.0000
3	-0.0067	+0.0111	1.0555
horn 3			
1	1.0580	-0.0344	+0.0250
2	-0.0004	1.0485	+0.0300
3	-0.0045	-0.0148	1.0489

horn 1			
1	**1.0300**	**-0.0350**	+0.0500
2	**0.0001**	**1.0641**	+0.0300
3	**0.0000**	-0.0258	1.0755
horn 2			
1	**1.0337**	**-0.0304**	0.0000
2	**0.0027**	**1.0435**	**-0.0144**
3	**-0.0006**	**+0.0211**	1.0555
horn 3			
1	**1.0420**	**-0.0326**	+0.0250
2	**0.0011**	**1.0328**	**+0.0215**
3	**0.0000**	-0.0148	1.0489

Table 1: APC matrix A. Version 2.0 (left). Version 3.0 (right). The A-matrix is written in Stokes components (I, Q, U). Aquarius does not measure the fourth component.

Table 1 lists the APC matrix A for V2.0 and the version used in V3.0. Changes are hi-lighted in red. The A-matrix transforms the portion of TA that comes from the Earth and atmosphere (i.e. TA after removing reflected signals from the Sun, Moon and celestial background; Section 3 of the ATBD) into a brightness temperature at the top of the ionosphere (TOI):

$$\mathbf{T}_{B,TOI} = \mathbf{A} \cdot \mathbf{T}_{A,Earth} \quad (1).$$

This A-matrix is based on a combination of the antenna pattern measured on the scale model with the most recent computed patterns obtained at JPL using GRASP software. The scale model patterns are used to model the spillover (off-Earth fraction) and the GRASP patterns are used for the Earth-view section and for the cross polarization correction. Adjustment in elements of the 3rd Stokes parameter (third row and third column) were made to reduce the biases that were observed over the ocean and the Amazon rain forest. For details of the derivation and validation of the V3.0 APC see the memo [*Meissner*, 2013].

2 Aquarius Wind Speeds

The surface roughness correction in V2.0 used NCEP GDAS wind speeds and the Aquarius scatterometer $\sigma_{0,VV}$ as input (see Section III of ATBD Addendum II) . For V3.0 wind speeds that are retrieved from Aquarius scatterometer and radiometer measurements [*Meissner et al.*, 2014] are being used.

Two Aquarius wind speed products are retrieved:

1. HH wind speeds, which use the scatterometer sigma0 at HH-pol.

2. HHH wind speeds, which use the scatterometer sigma0 at HH-pol and the radiometer TB at H-pol.

The retrieval for both wind speed products is based on a maximum likelihood estimate (MLE):

The sum of squares (SOS) in the MLE for the HH wind speed algorithm is:

$$\chi^2_{HH}(W) = \frac{\left[\sigma^{measured}_{0,HH} - \sigma^{GMF}_{0,HH}(W,\varphi_r)\right]^2}{\mathrm{var}\left(\sigma_{0,HH}\right)} + \frac{\left[W - W_{NCEP}\right]^2}{\mathrm{var}\left(W_{NCEP}\right)} \quad (2).$$

The SOS in the MLE for the HHH wind speed algorithm is:

$$\chi^2_{HHH}(W) = \frac{\left[\sigma^{measured}_{0,HH} - \sigma^{GMF}_{0,HH}(W,\varphi_r)\right]^2}{\mathrm{var}\left(\sigma_{0,HH}\right)} + \frac{\left[T^{measured}_{B,surf,H} - T^{GMF}_{B,surf,H}(W,\varphi_r)\right]^2}{\mathrm{var}\left(T_{B,surf,H}\right)} + \frac{\left[W - W_{NCEP}\right]^2}{\mathrm{var}\left(W_{NCEP}\right)} \quad (3).$$

The radar cross sections, $\sigma_0^{measured}$ are the values observed by the scatterometer at the top of the atmosphere and available in the L2 data file as scat_X_toa. The brightness temperature, $T_B^{measured}$ is the measure brightness temperature propagated to the surface (i.e. removing extraneous radiation and correcting for Faraday rotation and atmospheric attenuation) but with no correction for roughness. It is available in the L2 data file under the name rad_TbX. The forms of the geophysical model functions $\sigma^{GMF}_{0,HH}(W,\varphi_r)$ and $T^{GMF}_{B,surf,H}(W,\varphi_r)$ and the values of the expected variances $\mathrm{var}\left(\sigma_{0,HH}\right)$, $\mathrm{var}\left(T_{B,surf,H}\right)$, $\mathrm{var}\left(W_{NCEP}\right)$ are given in the appendices of this document. For additional information see [*Meissner et al.*, 2014].

For both the HH and HHH wind speed MLE we have found that assimilating the ancillary NCEP wind speed W_{NCEP} as background field into the MLE improves the skill at cross-wind observations, where the scatterometer cross section loses sensitivity. In both cases the wind direction φ_r is obtained from the ancillary NCEP GDAS field.

The GMF for the HHH wind speed (3) needs values for the SST and a 1st guess field for SSS as input. For SST we take the Reynolds (NCEP) 0.25° OI SST, which is already used as auxiliary input in the L2 algorithm. For the 1st guess auxiliary SSS field we have derived a climatology set of 12 monthly 2° maps that have been derived from the previous L2 processing V2.5.1. We have tested other 1st guess fields, e.g. the WOA climatology and found no significant difference between the final SSS retrievals. We have also tested an iterative procedure, which derives monthly SSS maps using HH wind speeds in the roughness correction and which does not need a 1st guess SSS input. Using those SSS maps as 1st guess in the HHH wind algorithm leads again to virtually the same result for the final SSS retrievals.

We have also tested that including the scatterometer VV-pol or the radiometer V-pol into the MLE (2) or (3) does not lead to a significant improvement in the performance of either wind speed product or the final SSS product. But note that the scatterometer VV-pol measurement $\sigma_{0,VV}$ is used in

the surface roughness correction together with the HHH wind speed (section 3); and the V-pol TB measurement is used in the salinity retrieval (section 4).

A validation study of the HH and HHH wind speeds [*Meissner et al.*, 2014] shows that the quality of the Aquarius HHH wind speeds matches those of WindSat and SSM/I. We estimate its overall accuracy to about 0.6 m/s. The overall accuracy of the HH wind speed is slightly less. Major degradation of the HH wind speeds occurs at higher winds (> 15 m/s) due to the loss of sensitivity of the scatterometer HH-pol cross section to wind speeds. The radiometer H-pol TB keeps its sensitivity to wind speed even in high winds [*Meissner et al.*, 2014].

In the L2 algorithm the HH wind speeds are used as auxiliary fields at stages where no well-calibrated radiometer measurement is yet available. This is the case for the calibration drift correction and also for the removal of reflected galaxy or solar radiation. The HHH wind speed is used in the final surface roughness correction (section 3).

For many observations with high land contamination (antenna pattern weighted land fraction > 0.1) or high sea ice contamination (antenna pattern weighted land fraction > 0.1) both the HH and HHH wind speed retrieval do not converge. If the land or sea ice fractions exceed 0.1, we do not retrieve HH or HHH wind speeds but use the NCEP wind speed in the surface roughness correction.

It should also be noted that the HH wind speed is different from the wind speed that is produced by the scatterometer algorithm [*Yueh et al.*, 2013], which uses both VV-pol and HH-pol scatterometer observations.

3 Surface Roughness Correction

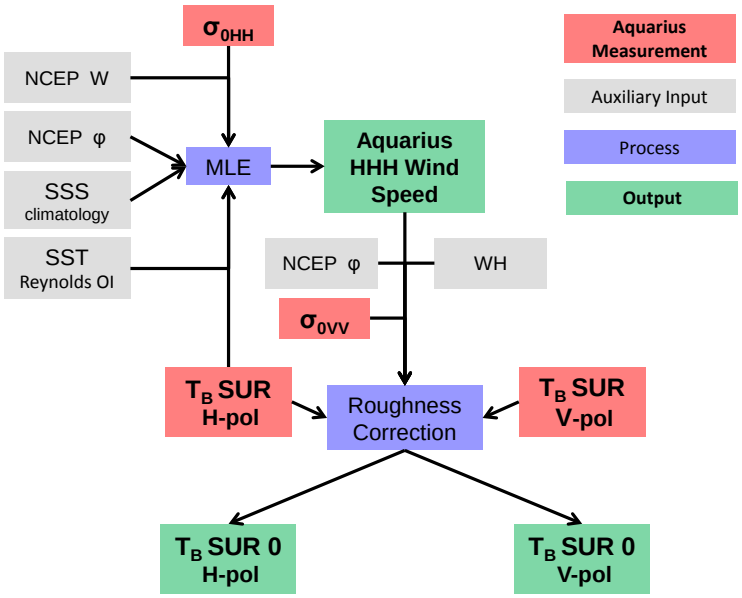

Figure 1: Flow chart of the V3.0 wind speed retrieval and surface roughness correction algorithms.

The form of the V3.0 surface roughness correction is:

$$\Delta E_{rough} = \Delta E_{W0}\left(W_{HHH}, \varphi_r, T_S\right) + \Delta E_{W1}\left(W_{HHH}, \sigma'_{0,VV}\right) + \Delta E_{W2}\left(W_{HHH}, SWH\right) \qquad (4).$$

In the GMF for the wind induced emissivity ΔE_{W0} we have introduced a dependence on SST as suggested in [*Meissner and Wentz*, 2012; Meissner et al., 2014]:

$$\Delta E_{W0,p} = \delta_p\left(W, \varphi_r\right) \cdot \frac{E_{0,p}\left(T_S\right)}{E_{0,p}\left(T_{ref}\right)} \qquad T_{ref} = 20^{\circ}C \qquad (5).$$

$E_0\left(T_S\right)$ is the specular surface emissivity. The model function for the form factor δ is an even 2nd order harmonic expansion in the relative wind direction φ_r :

$$\delta_p\left(W, \varphi_r\right) = A_{0,p}\left(W\right) + A_{1,p}\left(W\right) \cdot \cos\left(\varphi_r\right) + A_{2,p}\left(W\right) \cdot \cos\left(2 \cdot \varphi_r\right) \qquad (6).$$

The harmonic coefficients $A_{k,p}, k = 0,1,2$ depend on surface wind speed W, polarization p =V, H and EIA (i.e. different for each beam). $A_{k,p}\left(W\right)$ is fitted by a 5th order polynomial in W, which vanishes at W = 0:

$$A_{k,p}\left(W\right) = \sum_{i=1}^{5} a_{ki,p} \cdot W^i \qquad (7).$$

The values for $A_{k,p}\left(W\right)$ and the lookup tables $\Delta E_{W1}\left(W_{HHH}, \sigma'_{0,VV}\right)$ and $\Delta E_{W2}\left(W_{HHH}, SWH\right)$ are given in [*Meissner et al.*, 2014] and in Appendices C and D below. The coefficients are determined using one year of calibration data as described in Appendix A and in Meissner et al.. (2014).

As in Addendum II, the $\sigma'_{0,VV}$ in lookup table ΔE_{W1} is the observed VV-pol cross section after removing the wind direction signal:

$$\sigma'_{0,VV} \equiv \sigma^{meas}_{0,VV} - \left[B_{1,VV}\left(W_{HHH}\right) \cdot \cos\left(\varphi_r\right) + B_{2,VV}\left(W_{HHH}\right) \cdot \cos\left(2 \cdot \varphi_r\right) \right] \qquad (8)$$

See Appendix A for a description of the terms in brackets in Eqn 8. The significant wave height SWH in the lookup table ΔE_{W2} is taken from the NOAA/NCEP Wave Watch III model. Our data source is http://polar.ncep.noaa.gov/waves/download.shtml.

Figure 1 shows a flowchart of the V3.0 Aquarius HH and HH wind speed retrievals and surface roughness correction algorithms.

The following exceptions apply to the roughness correction:

1. NCEP wind speeds are used instead of HH/HHH wind speeds and only the 0th order term ΔE_{W0} in (4) is used if one of the following conditions applies:
    a. The scatterometer observation is missing or invalid.
    b. The scatterometer observation is flagged for RFI.
    c. The HH or HHH wind speed retrieval algorithm does not converge.

d. The 2-dimensional lookup table for the 1st order term $\Delta E_{W,1}$ in (4) is underpopulated for either the HH or the HHH wind speeds.

When this occurs, the same emissivity model function $\Delta E_{W,0}\left(W,\varphi_r,T_S\right)$ is used that was derived for the HH/HHH wind speeds but with W_{NCEP} instead of W_{HH} or W_{HHH}. A Q/C flag is set accordingly [*LeVine and Meissner*, 2014].

2. If the value for the SWH is missing or invalid then $\Delta E_{W,2}$ in (4) is set to 0 and the series in (4) is terminated after the 1st order term $\Delta E_{W,1}$. A Q/C flag is set accordingly [*LeVine and Meissner*, 2014].

4 Salinity Retrieval

The V3.0 salinity retrieval uses both V-pol and H-pol surface TB. In V2.0 we had used only the V-pol.

The outputs of the surface roughness correction algorithm (section 3) are ocean surface brightness temperatures for V-pol and H-pol that are referenced to a flat ocean surface $T_{B,spec,P}^{measured}$, where P=V-pol or H-pol. (This is rad_TbX_rc in the L2 data file.) These measured values are matched to values computed assuming a flat ocean surface using the Fresnel reflection coefficients with the Meissner-Wentz model for the dielectric constant of sea water [*Meissner and Wentz,* 2004, 2012; Meissner et al., 2014]. The brightness temperature, $T_{B,spec,P}^{RTM}$, obtained in this manner is identical to multiplying the specular emissivity $E_0\left(T_S\right)$ by the surface temperature T_S . The matching in the V3.0 salinity retrieval is done by a maximum likelihood estimate, whose SOS reads:

$$\chi^2=\frac{\left[T_{B,spec,V}^{measured}-T_{B,spec,V}^{RTM}\left(T_S,SSS\right)\right]^2}{\mathrm{var}\left(T_{B,spec,V}\right)}+\frac{\left[T_{B,spec,H}^{measured}-T_{B,spec,H}^{RTM}\left(T_S,SSS\right)\right]^2}{\mathrm{var}\left(T_{B,spec,H}\right)} \qquad (9).$$

To obtain values for the expected variances in (9) we have computed the standard deviations between the measured and expected $T_{B,spec}$ for each 1.44 sec interval and for one year, where in the computation of the expected (i.e. RTM) $T_{B,spec}$ the HYCOM SSS field was used. The values of the standard deviations are listed in Table 2 for the various channels. Their squares (variance) are the inverse of the weights used in Eqn (9) . They are static parameters and do not change.

Channel	1V	1H	2V	2H	3V	3H
expected standard deviation [K]	0.265	0.220	0.282	0.209	0.288	0.205

Table 2: Expected standard deviation (square roots of the inverse of the channel weights) in the MLE (9).

The goodness of fit in the MLE can be characterized by the root sum of squares of measured minus calculated TB, where in the RTM calculation the actual retrieved Aquarius salinity is used. We call this parameter T_{Berr} or $T_{B\ consistency}$.

$$T_{B,err} = \sqrt{\left[T_{B,spec,V}^{measured} - T_{B,spec,V}^{RTM}\left(T_S, SSS_{AQ}\right)\right]^2 + \left[T_{B,spec,H}^{measured} - T_{B,spec,H}^{RTM}\left(T_S, SSS_{AQ}\right)\right]^2} \qquad (10)$$

Large values for T_{Berr} indicate a poor fit between observation (note: T_{Berr} is called rad_Tb_consistency in the L2 data file). This can be caused for example by undetected RFI, contamination from land, sea ice or celestial radiation that has not been properly removed. We use the value of T_{Berr} as a quality control (Q/C) indicator for the salinity retrievals [*Meissner*, 2014].

5 Reflected Galactic Radiation

5.1 Ascending – Descending Biases in Aquarius V2.0

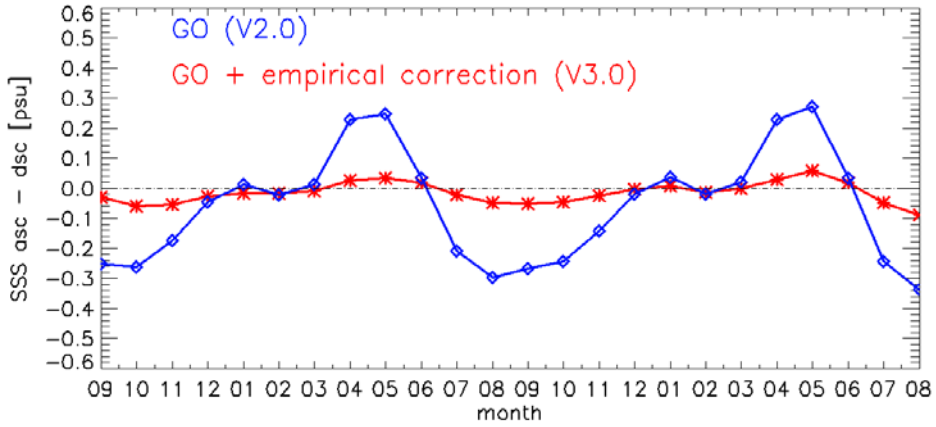

Figure 2: Global monthly salinity differences between ascending and descending swaths: V2.0, which uses the GO optics model for calculating the reflected galactic radiation (blue curve). V3.0, which adds an empirical symmetrization correction (red curve).

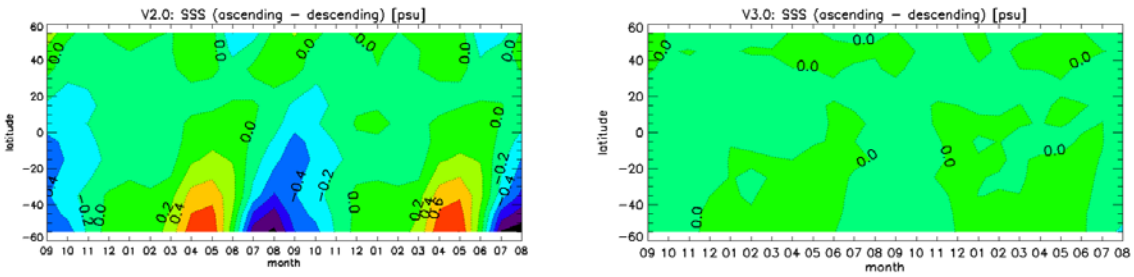

Figure 3: Hovmoeller plot of the monthly salinity difference between ascending and descending Aquarius swaths. The x-axis is time (months since September 2011) and the y-axis is latitude. Left panel: Using the geometric optics (GO) model for calculating the reflected galactic radiation (V2.0). Right panel: After adding the empirical symmetrization correction (V3.0).

The Aquarius V2.0 salinity fields show significant differences between ascending (evening) and descending (morning) swaths (blue curve in Figure 2, left panel in Figure 3), which cannot be justified physically large and therefor are regarded as spurious. These ascending – descending biases have a clear spatial and temporal pattern (left panel in Figure 3) which strongly correlates with the reflection of galactic radiation from the ocean surface (L2-ATBD, section 2.2.2 and Appendix A).

The algorithm in V2.0 for correcting for the reflected galactic radiation $\mathbf{T}_{A,gal,ref}$ was developed pre-launch (i.e. before seeing the data) using a geometric optics (GO) model for reflection from the surface. The ocean surface is modeled as an ensemble of tilted facets, from which the galactic radiation is reflected. The slope probability density function for the titled facets was assumed to be Gaussian as described in Appendix A of the L2-ATBD.

The reflected galactic radiation can be as high as 5 K (for the average of V-pol and H-pol), which corresponds to a signal of 10 psu in salinity. Figure 3 shows that the residual salinity error reaches 1.0 psu. That means that the GO model in V2.0 correctly removes most (about 90%) of the reflected galactic radiation. Nevertheless, the size of the residual errors (Figure 2 and 3) is large enough to warrant some adjustments to the galaxy correction.

5.2 Need for an Empirical Correction for the Reflected Galaxy

There are several reasons why inaccuracies in the GO treatment can arise:

1. The value of the variance of the slope distribution (equation A11 in Appendix A of the L2-ATBD) is not completely correct;
2. The GO model assumes an isotropic (independent of direction) slope distribution, which does not account for wind direction effects;
3. There are other ocean roughness effects, which cause reflection of galactic radiation but cannot be modeled with an ensemble of tilted facets (e.g. Bragg scattering at short waves, breaking waves and/or foam, net directional roughness features on a large scale);
4. The galactic tables themselves, which were derived from radio astronomy measurements [*LeVine and Abraham*, 2004] could have inaccuracies (most likely associated with strong sources near the galactic plane).

All those effects are very difficult or impossible to model. We have therefore decided to derive and use a purely empirical correction for the reflected galactic radiation, which is added to the GO calculation. The danger in doing this is that other geophysical issue (i.e. not associated with reflected radiation from the galaxy) could be masked. But, it was decided to accept this risk for V3.0. The Aquarius science team will continue to review the issue looking for refinements.

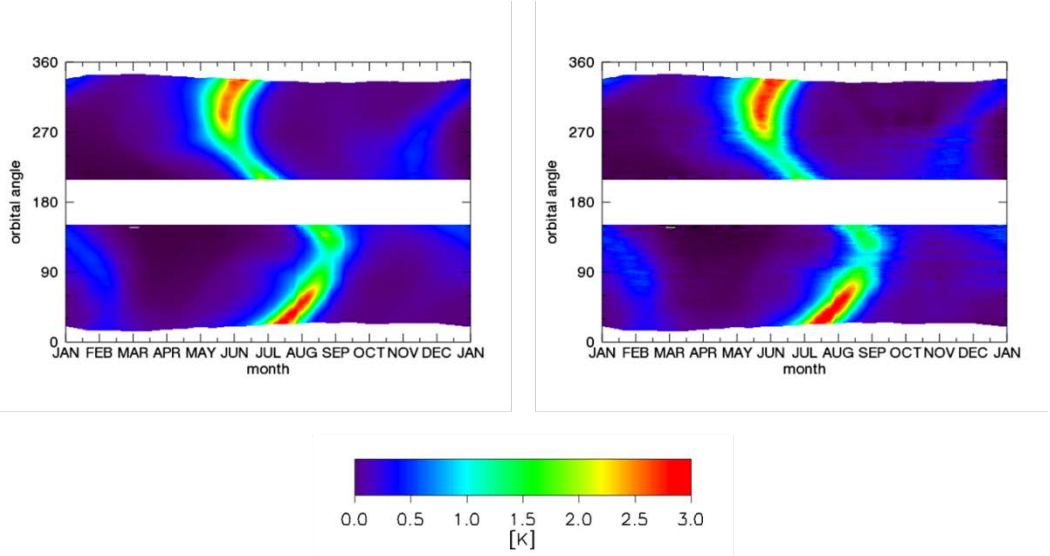

Figure 4: TA galactic reflected (average of V and H pol) for Aquarius horn 3. Left: GO (V2.0), right: after adding the empirical correction (V3.0). The x-axis is time of the sidereal year. The y-axis is the orbital position angle (z-angle).

This empirical correction is based on symmetrizing the ascending and the descending Aquarius swaths. The size of the correction is about 10% of the GO calculation. The correction before (GO only) and after the symmetrizing is shown in Figure 4. Figure 2 and Figure 3 show that adding this empirical term to the GO calculation improves the ascending - descending biases significantly.

In the following we spell out the details of the derivation of this empirical correction.

5.3 Empirical Correction: Basis Assumptions

The basic assumptions are:

1. There are no zonal ascending – descending biases in ocean salinity on weekly or larger time scales.
2. The residual zonal ascending – descending biases that are observed in V2.0 are all due to the inadequacies (either over or under correction) in the GO model calculation for the reflected galactic radiation.
3. The size of the residual ascending – descending biases is proportional to the strength of the reflected galactic radiation.

Assumption 1 is based on current understanding of the structure of the salinity field for which there no known physical processes that would cause such a difference. Assumption 2 results from analyses of the V2.0 salinity fields and known limitation of the GO model. Assumption 3 is based on theory for scattering from rough surfaces and the fact that the source and surface are independent. It is expected to hold in some mean sense over the footprint.

5.4 Zonal Symmetrization Procedure

A symmetrization of the ascending and descending Aquarius swaths is done on the basis of a zonal average. According to assumption 3 above (Section 5.3) the symmetrization weights will be determined by the strength of the reflected galactic radiation.

For the time being, only the 1st Stokes parameter I = (Tv+ Th) is considered which is the sum of the brightness temperatures at the ocean surface and will be denoted by T_B. In the equations below, $\langle \ldots \rangle$ denotes the zonal average and the variable z denotes the orbital angle (z-angle). If z lies in the ascending swath, then $-z$ (or $360^\circ - z$) lies in the descending swath and vice versa. $T_B(z)$ is first Stokes parameter as measured by Aquarius at the surface at z . $T_{A,gal,ref}(z)$ is the value of the reflected galactic radiation received by Aquarius as computed in the GO model. The symmetrization term, $\Delta(z)$, which is the basis of the empirical correction, is given as:

$$\Delta(z) = \left[p \cdot \langle T_B(z) \rangle + q \cdot \langle T_B(-z) \rangle \right] - \langle T_B(z) \rangle$$

$$p = \frac{\langle T_{A,gal,ref}(-z) \rangle}{\langle T_{A,gal,ref}(z) \rangle + \langle T_{A,gal,ref}(-z) \rangle} \qquad (11).$$

$$q = \frac{\langle T_{A,gal,ref}(z) \rangle}{\langle T_{A,gal,ref}(z) \rangle + \langle T_{A,gal,ref}(-z) \rangle}$$

The probabilistic channel weights p and q add up to 1: $p+q=1$. The symmetrized surface T_B called T_B' is given by:

$$T_B'(z) \equiv T_B(z) + \Delta(z) \qquad (12).$$

It is not difficult to see that this symmetrization has the following features:

1. Assume that z lies in the ascending swath and therefore $-z$ lies in the descending swath. If there is no reflected galactic radiation in the ascending swath, i.e. $\langle T_{A,gal.ref}(z) \rangle = 0$, then $p=1$ and $q=0$. That means that the symmetrization term and thus the whole empirical correction $\Delta(z)$ vanishes, and therefore: $T_B'(z) = T_B(z)$.
2. If, on the other hand, there is no reflected galactic radiation in the descending swath, i.e. $\langle T_{A,gal.ref}(-z) \rangle = 0$, then $p=0$ and $q=1$. That implies $\Delta(z) = \langle T_B(-z) \rangle - \langle T_B(z) \rangle$ and thus $\langle T_B'(z) \rangle = \langle T_B(-z) \rangle$.
3. The zonal average of T_B' is symmetric: $\langle T_B'(z) \rangle = \langle T_B'(-z) \rangle$.

4. If the reflected galactic radiation is the same in ascending and descending swaths $\left\langle T_{A,gal.ref}\left(z\right)\right\rangle = \left\langle T_{A,gal.ref}\left(-z\right)\right\rangle$, then $p = q = \frac{1}{2}$ and thus the global average (sum of ascending and descending swaths) does not change after adding the symmetrization term: $\left\langle T_B{}'\left(z\right)\right\rangle + \left\langle T_B{}'\left(-z\right)\right\rangle = \left\langle T_B\left(z\right)\right\rangle + \left\langle T_B\left(-z\right)\right\rangle$.
5. If the zonal T_B averages are already symmetric $\left\langle T_B\left(z\right)\right\rangle = \left\langle T_B\left(-z\right)\right\rangle$, then the symmetrization term and thus the whole empirical correction $\Delta\left(z\right)$ vanishes, and therefore: $T_B{}'\left(z\right) = T_B\left(z\right)$. That means that we do not introduce any additional ascending – descending biases that were not already there.

An important feature of this symmetrization procedure is the fact that it is derived from Aquarius measurements only and does not rely on or need any auxiliary salinity reference fields such as HYCOM.

5.5 Correction Algorithm for the Reflected Galactic Radiation

In the L2 algorithm, the correction for the galaxy radiation (L2ATBD section 2.2.2 and Appendix A) is done at the TA rather the TB level. The symmetrization correction Δ for the 1st Stokes was derived at the TB level. It can be lifted to the TA level by dividing it by the spillover factor, which is the II component of the APC matrix (section 1):

$$\Delta_{A,I}\left(z\right) \approx \frac{\Delta_I\left(z\right)}{A_{II}} \tag{13}.$$

It is assumed that the galactic radiation itself is unpolarized and polarization occurs only through the reflection at the ocean surface. Ignoring Faraday rotation of the galactic radiation in the empirical correction term, its 2nd and 3rd Stokes component are:

$$\begin{aligned} \Delta_{A,Q} &\approx \frac{R_V - R_H}{R_V + R_H}\cdot\Delta_{A,I} \approx \frac{T_{A,gal,ref,Q}}{T_{A,gal,ref,I}}\cdot\Delta_{A,I} \\ \Delta_{A,U} &\approx 0 \end{aligned} \tag{14}.$$

In (14) $R_{V,H}$ are the reflectivity for V and H polarization of an ideal (i.e. flat) surface. In the correction algorithm the reflected galactic radiation is subtracted from the measured $\mathbf{T}_A$ to get the contribution $\mathbf{T}_{A,Earth}$ that comes from the Earth only. This means that the full correction for the reflected galactic radiation in V3.0 is given by:

$$\mathbf{T_{A,gal,ref,P}} = \mathbf{T^{GO}_{A,gal,ref,P}} - \mathbf{\Delta_{A,P}} \quad P = I,Q,U \tag{15}$$

In (15) $\mathbf{T^{GO}_{A,gal,ref,P}}$ is the GO optics term, which is used in V2.0.

In the implementation of the empirical correction in the algorithm code, the term $\mathbf{\Delta}_{\mathbf{A,P}}$ is cast in form of a lookup table as is done for $\mathbf{T}^{\mathbf{GO}}_{\mathbf{A,gal,ref,P}}$ itself (section 2.2.2 of the L2ATBD). The dimensions of the lookup table for $\mathbf{\Delta}_{\mathbf{A,P}}$ are (1441, 1441, 3,3), referring to time of the sidereal year, orbit position (z-angle), polarization (Stokes number) and radiometer (horn) number. We have not stratified the empirical correction $\mathbf{\Delta}_{\mathbf{A,P}}$ by wind speed and therefore the lookup table does not have a wind speed dimension. For the derivation of the lookup table we have used 2 years of Aquarius measurements from September 2011 – August 2013.

6 Salinity Bias Adjustment

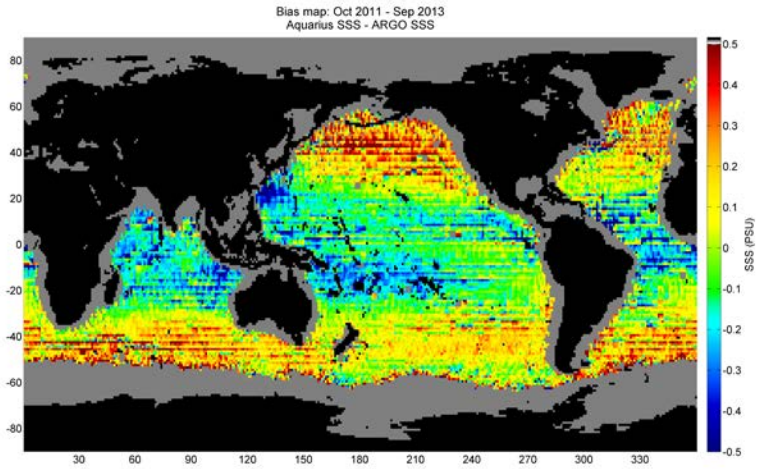

Figure 5: Mean SSS bias for Oct 2011 to Sep 2013 for the Aquarius standard SSS compared to gridded ADPRC (University of Hawaii) ARGO salinity. The data are resampled to one-degree, monthly map. The monthly SSS difference is then averaged over the two-year time period.

Regional biases have been discovered when comparing Aquarius SSS derived with SSS from HYCOM, and ARGO. These biases were noticed in Level 3 difference maps using data resampled to one degree spatial resolution and averaged over the two-year period, Oct 2011 to Sep 2013. The differences were observed when comparing to either HYCOM as well as ARGO salinity (Figure 5). Positive biases exceeding 0.4 psu are noticed in mid-high latitudes, and negative biases as low as – 0.4 psu are noticed in the tropics and sub-tropics.

The zonal character of those biases evident in Figure 5 suggest that they are correlated with SST. This is confirmed when the differences are plotted as a function of SST. The reason for the bias is not known at this time, but is likely caused by residual errors in the geophysical model function that is used in the SSS retrieval algorithm. The most probable candidates to cause SST dependent errors in the geophysical model function are the model for the dielectric constant and the model for atmospheric absorption and emission. The effect of surface roughness could also have an SST dependence which is currently not correctly included in the current correction. Most likely it is a

combination of error sources. The magnitude of the observed SSS biases translates into a radiometric error of the order of 0.2 K. On that level it is very difficult to disentangle the various terms in the geophysical model function and adjust them individually

Rather than leave the SST dependent bias in the data, it was decided to provide the user with both a standard product and one with the bias removed. The standard product will help users interested in looking into the cause of the bias and the adjusted SSS will help users only interested in the best estimate of SSS available at this time.

A correction for the SST dependent bias has been generated using the HYCOM SSS as a reference. The difference between the SSS retrieved by Aquarius using V3.0 and the SSS from HYCOM has been averaged into monthly 1 deg maps. The same is done for the auxiliary SST field. The differences from all 3 Aquarius horns are averaged to obtain a single correction. Any Aquarius observation that is degraded according to one of the moderate-level quality control checks listed in LeVine and Meissner (2014) has been discarded. The data have also been screened to rule out freshening effects of rain. This was done taking observations from the CONAE MWR Ku-band radiometer, which can be space-time collocated to the Aquarius measurements and which allows retrieval of the surface rain rate at the location and instance of Aquarius (Biswas et al., 2012).

The form of the adjustment was obtained by fitting a quadratic function in SST to the observed Aquarius – HYCOM SSS differences. The result is:

$$\begin{aligned} SSS_{bias\_adj} &= SSS_{Aq} - \Delta SSS_{bias\_adj}\left(T_S\right) \\ \Delta SSS_{bias\_adj}\left(T_S\right) &= -0.0019594 \cdot T_S{}^2 + 1.1257 \cdot T_S - 161.4934 \end{aligned} \tag{16}$$

SSS_{Aq} is the standard L2 Aquarius SSS product. The units of sea surface temperature T_S are in Kelvin. The unit of ΔSSS_{bias_adj} are psu. The adjustment (16) is the same for all 3 Aquarius horns. The functional dependence $\Delta SSS_{bias\_adj}\left(T_S\right)$ is shown in Figure 6.

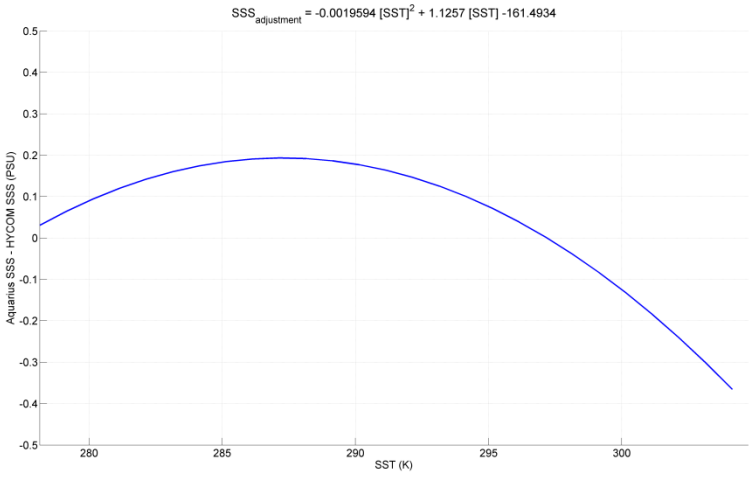

Figure 6: Functional form of the adjustment for dependence on SST. In the derivation of equation (16) cold water $T_S < 5^\circ C$ has been excluded. However, the adjustment seems to also work in cold water and seems to work down to $T_S = 0^\circ C$. Therefore equation (16) is used for all SST.

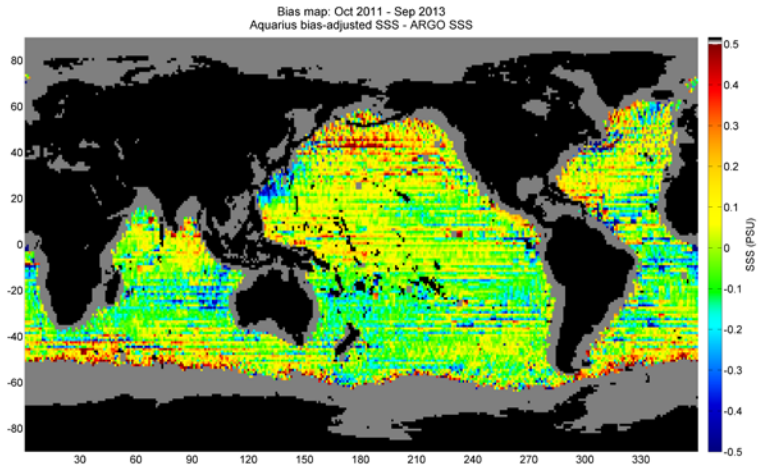

Figure 7: Mean SSS bias for Oct 2011 to Sep 2013 using the adjusted Aquarius SSS. As in Figure 5, the data are resampled to a one-degree, monthly SSS difference and then averaged over the two-year time period. The difference is between adjusted Aquarius SSS and SSS from ARGO (ADPRC, University of Hawaii).

Figure 7 shows the difference after correction.

The Aquarius V3.0 L2 and L3 files contain both the standard Aquarius SSS retrieval SSS_{Aq} and the post-hoc corrected product SSS_{bias_adj} .

7 Drift Correction

The approach used to mitigate the radiometer drift has been modified. A detailed description of the procedure for radiometer calibration in V3.0 is given in Appendix E.

The drift is still divided into two parts (Addendum II), an exponential and wiggles. The exponential is treated as a gain drift and the wiggles are now treated as an offset (bias).

7.1. The exponential is unchanged. An exponential if fitted to the monotonic change in each radiometer channel (TF – TA_exp where TA is rad_exp_TaX in the L2 data file). A global average has been computed weekly for the history of the mission and used to establish the decay constant (ex-ponent) for the exponential for each channel (polarization and radiometer). These numbers have remained stable but are continued to be checked weekly. If new data warrants a change, the expo-nent will be adjusted.

The exponential portion of the drift is treated as a gain drift. This was established by comparing the drift over different scenes (e.g. land and ocean). A gain drift should scale with the scene temperature and a bias should be independent of the scene. The change in gain indicated by the expo-

nential component of the instrumental drift is corrected by adjusting the temperature of the Aquarius reference noise diode. This temperature is changed enough to cause the required change in gain.

As of this note, the exponential continues to "flatten" and the changes in gain are small.

7.2. The method for treating the wiggle correction has been modified. The regional singular value decomposition adopted in Addendum II and used in V2.0 has been abandoned for a simple 7-day average. The difference, TF – TA_exp, is computed globally (average value globally computed every 7-day repeat cycle). A correction is made for the exponential drift. Then the residual (wiggle) is removed. This residual is treated like a bias. That is, it is subtracted as a constant from each radiometer channel.

7.3. Calibration Data: When making the adjustments described above, a subset of data designated for use for calibration is used. This is defined by a series of L2 masks and described in the L2 product specification document (see Table I). Also see [Meissner, 2014], .

7.4. Flags: The flags for L2 data have been revised and new flags added. See AQ-014-PS-0006 for details. In addition a subset of the flags has been identified to be used as masks to define data to be used for L2 calibration where a more restrictive set of data is desired. These same flags are used but at a lower level of exclusion to mask data transferred from L2 to L3. See AQ-014-PS-0006 and the notes below Table I in the product specification document for additional details.

8 References

S. Biswas, L. Jones, D. Rocca and J.-C. Gallio (2012), Aquarius/SAC-D Microwave Radiometer (MWR): Instrument description & brightness temperature calibration, IGARSS 2012, doi: 10.1109/IGARSS.2012.6350705.

D. LeVine and S. Abraham (2004), Galactic noise and passive microwave remote sensing from space at L-band, IEEE Trans. Geosci. Remote Sens., 42 (1), 119-129.

D. LeVine and T. Meissner (2014), Proposal for Flags and Masks, AQ-014-PS-0006, February 2014.

T. Meissner and F. Wentz (2004), The complex dielectric constant of pure and sea water from microwave satellite observations, IEEE Trans. Geosci. Remote Sens., 42(9), 1836-1849.

T. Meissner and F. Wentz (2012), The emissivity of the ocean surface between 6 and 90 GHz over a large range of wind speeds and earth incidence angles, IEEE Trans. Geosci. Remote Sens., 50(8), 3004-3026.

T. Meissner (2013), Memo: Proposed APC Changes from V2.0 to V3.0, 05/19/2013, RSS Tech. Report 05192013.

T. Meissner (2014), Memo: Performance Degradation and Q/C Flagging of Aquarius L2 Salinity Retrievals, 01/20/2014, RSS Tech. Report 01202014, Version 3.

T. Meissner, F. Wentz and L. Ricciardulli (2014), A geophysical model for the emission and scattering of L-band microwave radiation from rough ocean surfaces, submitted to JGR Ocean Special Section Early scientific results from the salinity measuring satellites Aquarius/SAC-D and SMOS, manuscript no. 2014JC009837, http://www.remss.com/about/profiles/thomas-meissner.

S. Yueh et al. (2013), Aquarius Scatterometer Algorithm Theoretical Basis Document, avail JPL PO.DAAC: http://podaac.jpl.nasa.gov/aquarius

9 Appendix A: Scatterometer Model Function $\sigma_{0,p}^{GMF}(W,\varphi_r)$

The geophysical model functions for the scatterometer σ_0 can be expanded into a Fourier series of even harmonic functions in the relative wind direction, φ_r [*Wentz*, 1991; *Isoguchi and Shimada*, 2009; *Yueh et al.*, 2010]. Keeping terms up to 2nd order:

$$\sigma_{0,p}^{GMF}(W,\varphi_r) = B_{0,p}(W) + B_{1,p}(W)\cdot\cos(\varphi_r) + B_{2,p}(W)\cdot\cos(2\cdot\varphi_r) \qquad \text{(A1)}$$

where W is the surface wind speed and p =VV, HH, VH, HV is the scatterometer polarization. The coefficients, $B_{k,p}$, depend on incidence angle (and polarization) and therefore are different for each scatterometer channel. The coefficients are B(W) are expressed as a 5th order polynomial in W:

$$B_{k,p}(W) = \sum_{i=1}^{5} b_{ki,p}\cdot W^i \qquad \text{(A2)}$$

where the sum is over i = {1…5}.

In (A1) the wind direction, $\varphi_r = \varphi_w - \alpha$ where φ_w is the geographical wind direction relative to North and α is the azimuthal direction. An upwind observation has $\varphi_r = 0°$, a downwind observation has $\varphi_r = 180°$ and crosswind observations have $\varphi_r = +/-90°$. The value for φ_w comes from the ancillary NCEP GDAS field.

The coefficients $b_{k,p}$ are determined from the Aquarius data using a subset of data selected for quality and the presence of the required ancillary data (i.e. wind speed and direction). For this purpose a match-up data set has been created of Aquarius brightness temperatures and scatterometer σ0 with microwave imager wind speeds, W, from the Level 3 Remote Sensing Systems (RSS) Version 7 climate data record (www.remss.com). For a valid match-up a wind speed measurement from either WindSat or F17 SSMIS is required to exist no more than 1 hour from the Aquarius observation and with the center of the Aquarius footprint within the 1/4° by 1/4° cell of the L3 wind speed map. In addition, an observation is discarded if any of the following quality control (Q/C) conditions applies:

1. The antenna pattern weighted land or ice fraction within the Aquarius footprint exceeds 0.001.

2. The L2 Aquarius data product flags the scatterometer observation for RFI [*Yueh et al.*, 2012].

3. The L2 Aquarius data product indicates possible RFI contamination of the radiometer defined as |TF - TA| > 1.0K

4. The radiometer observation falls within areas in which data analysis indicates anamolies that suggest contamination (perhaps by RFI) as outlined in Section 2.9 of RSS Tech Report 01202014 *[Meissner, 2014]* (see Figure 8).

5. The L2 Aquarius data product indicates degraded navigation accuracy or if there is an spacecraft maneuver (Flag 16, pointing anomaly, set).

6. The RSS L3 map indicates rain within the 1/4° by 1/4° grid cell or any of its 8 surrounding 1/4° by 1/4° grid cells.

7. The value for the average of V-pol and H-pol of the galactic radiation that is reflected from a specular ocean surface exceeds 1.5 K.

If there is a valid match-up wind speed for both WindSat and F17 SSMIS, only the WindSat observation is included in the match-up set.

The match-up data set used comprises the full calendar year 2012. The total number of match-ups is about 5 million for each of the three Aquarius horns. The match-up data is binned (averaged) into 2-dimensional intervals (W, φr), whose sizes are 1 m/s for W and 10° for φr.

This data used to derive the GMF for sigma0 is not the same as the calibration data set defined for use with V3.0 (see the Table I in the L2 data specification document for V3.0). It is believed that the GMF is sufficiently accurate that a change was not warranted when the new masks for the calibration data for V3.0 were established.

radiometer 1 VV b 0i		radiometer 2 VV b 0i		radiometer 3 VV b 0i	
1	2.7669953402e-002	1	1.2863352200e-002	1	7.9812841854e-003
2	-3.5648121980e-003	2	-2.0993592491e-003	2	-1.4250014823e-003
3	2.5085738933e-004	3	1.6518875147e-004	3	1.1846924116e-004
4	-7.6604470290e-006	4	-5.4682006056e-006	4	-4.0865529161e-006
5	8.3403936421e-008	5	6.4132838313e-008	5	4.9691503580e-008

radiometer 1 HH b 0i		radiometer 2 HH b 0i		radiometer 3 HH b 0i	
1	1.2755914080e-002	1	3.7572819799e-003	1	1.4664950940e-003
2	-1.1566306028e-003	2	-5.3258749393e-004	2	-2.4374331007e-004
3	7.5880134855e-005	3	4.3724484672e-005	3	2.1823161004e-005
4	-2.1193397012e-006	4	-1.4681802479e-006	4	-7.7367920090e-007
5	1.9732074898e-008	5	1.7169850326e-008	5	9.4709584062e-009

radiometer 1 VV b 1i		radiometer 2 VV b 1i		radiometer 3 VV b 1i	
1	3.1471932686e-004	1	5.2348832960e-004	1	2.8558723483e-004
2	-1.0708873066e-004	2	-2.0409803674e-004	2	-1.1332749701e-004
3	9.8366727292e-006	3	2.6073582526e-005	3	1.4903721848e-005
4	-1.5828345752e-007	4	-1.1566411871e-006	4	-6.4922700321e-007
5	-2.3597221602e-009	5	1.7537140274e-008	5	9.4205608577e-009

radiometer 1 HH b 1i		radiometer 2 HH b 1i		radiometer 3 HH b 1i	
1	3.6370936768e-004	1	3.3829156489e-004	1	1.2856275234e-004
2	-1.1753728728e-004	2	-1.3147938974e-004	2	-5.0136994111e-005
3	1.3593095709e-005	3	1.8137648631e-005	3	7.3669264038e-006
4	-3.4977915542e-007	4	-7.9436180922e-007	4	-3.1710126109e-007
5	8.1882224455e-010	5	1.1628671488e-008	5	4.4180628101e-009

radiometer 1 VV b 2i		radiometer 2 VV b 2i		radiometer 3 VV b 2i	
1	1.9129701422e-003	1	5.5889743658e-004	1	4.4372478525e-004
2	-1.4546678790e-003	2	-5.0187584565e-004	2	-3.1164511936e-004
3	2.1484907649e-004	3	7.9280278992e-005	3	4.9980678917e-005
4	-9.9712358461e-006	4	-3.6902553692e-006	4	-2.3909290707e-006
5	1.5136841055e-007	5	5.4847783328e-008	5	3.6603560390e-008

radiometer 1 HH b 2i		radiometer 2 HH b 2i		radiometer 3 HH b 2i	
1	1.5807451212e-003	1	3.7371603939e-004	1	1.5707164701e-004
2	-9.5377945712e-004	2	-2.4023678467e-004	2	-9.3649029302e-005
3	1.3424379381e-004	3	3.4716850703e-005	3	1.3860196514e-005
4	-6.0496459000e-006	4	-1.5485629837e-006	4	-6.3232563194e-007
5	8.9841023600e-008	5	2.2414676330e-008	5	9.3928175374e-009

Figure A1: The coefficients $b_{k,p}$ in Eqn A2. These are also available in a text file (Meissner, 2014)

10 Appendix B: Radiometer Model Function $T_{B,surf,P}^{GMF}$

The model function for the brightness temperature at the surface is the sum of the value from an ideal (i.e. flat and homogenous) surface plus a contribution from roughness. The portion for the flat surface is obtained using the Fresnel reflection coefficients: $T_B = \left(1-\rho^2\right)\cdot T_S$ where ρ is the Fresnel reflection coefficient and Ts the physical temperature of the surface. This brightness temperature is called $T_{B,spec,P}^{RTM}$ in Eqn (9) where it is computed using the Meissner-Wentz model for the dielectric constant of sea water. The roughness correction is obtained by multiplying ΔE_{rough} in Eqn (i.e. ΔE_{W0}) by the surface temperature. Thus:

$$T_{B,surf,P}^{GMF} = T_{B,spec,P}^{RTM} + \Delta E_{rough}\cdot T_S \qquad \text{(B1)}$$

where $T_{B,spec,P}^{RTM}$ is as given in Eqn 8 and Ts is the physical temp of the surface. Only the first order term, ΔE_{W0}, in the roughness correction derived in Section 3 is used in the model function for deriving winds. This is good enough for retrieving the HHH wind speeds. The higher order terms (ΔE_{W1} and ΔE_{W2}) are small. But doing the roughness correction itself in the retrieval (i.e. correcting TB, all the terms in Eqn 4 are used.

11 Appendix C: Coefficients for Emissivity Model Function: $A_{k,p}$

The dominant term in the expression for the change in emissivity due to sea surface roughness (Eqn (4)) is proportional to (Eqn 5 and 6):

$$\delta_p(W,\varphi_r) = A_{0,p}(W) + A_{1,p}(W)\cdot\cos(\varphi_r) + A_{2,p}(W)\cdot\cos(2\cdot\varphi_r) \qquad \text{(C1)}$$

where φ_r is the wind direction. The harmonic coefficients $A_{k,p}, k = 0,1,2$ depend on surface wind speed W, polarization p =V,H and local angle of incidence (i.e. different for each beam). Each $A_{k,p}(W)$ is fitted by a 5th order polynomial in W, which vanishes at W = 0:

$$A_{k,p}(W) = \sum_{i=1}^{5} a_{ki,p}\cdot W^i \qquad \text{(C2)}$$

The coefficients $\alpha_{ki,p}$ are determined using one year of the calibration data described in Appendix A and also in Meissner et al. (2014). The coefficients $\alpha_{ki,p}$ are listed below in Figure C1and a text file with the coefficients is in [*Meissner et al.., 2014*].

radiometer 1		radiometer 2		radiometer 3	
V		V		V	
a 0i		a 0i		a 0i	
1	5.7894060320e-001	1	5.0281588143e-001	1	4.7027203005e-001
2	-1.0473595790e-001	2	-8.4035755450e-002	2	-7.6334662983e-002
3	9.9200140518e-003	3	7.8518455026e-003	3	6.9857495929e-003
4	-3.6291757411e-004	4	-2.8030380618e-004	4	-2.4303426684e-004
5	4.6589912401e-006	5	3.5109805876e-006	5	2.9390853226e-006

radiometer 1		radiometer 2		radiometer 3	
H		H		H	
a 0i		a 0i		a 0i	
1	7.7153019419e-001	1	8.4965177001e-001	1	1.0601673642e+000
2	-1.2715188465e-001	2	-1.2443856200e-001	2	-1.4677107298e-001
3	1.1329089683e-002	3	1.0359930394e-002	3	1.1480019211e-002
4	-4.0789149957e-004	4	-3.5549109274e-004	4	-3.8084012081e-004
5	5.2183370672e-006	5	4.3636667626e-006	5	4.5485097434e-006

radiometer 1		radiometer 2		radiometer 3	
V		V		V	
a 1i		a 1i		a 1i	
1	2.1216534279e-002	1	1.5596703582e-003	1	9.1197181127e-003
2	-7.1813519762e-003	2	2.3582984624e-003	2	-3.0431623312e-003
3	9.1738225933e-004	3	-3.4662668911e-004	3	5.0839571367e-004
4	-3.9535822500e-005	4	2.6606348124e-005	4	-2.0375986729e-005
5	5.6502242949e-007	5	-6.1842609629e-007	5	2.4580823525e-007

radiometer 1		radiometer 2		radiometer 3	
H		H		H	
a 1i		a 1i		a 1i	
1	3.3306056615e-003	1	-1.8863269506e-002	1	9.6160121528e-003
2	-3.7204789320e-003	2	6.5676785996e-003	2	-4.3505334225e-003
3	6.2494297864e-004	3	-7.3111819961e-004	3	6.0718079191e-004
4	-3.2678064089e-005	4	3.7255111733e-005	4	-2.7536464802e-005
5	5.3603866560e-007	5	-6.8989289663e-007	5	4.0733177632e-007

radiometer 1		radiometer 2		radiometer 3	
V		V		V	
a 2i		a 2i		a 2i	
1	6.6222103677e-002	1	5.1196349082e-002	1	9.3408423686e-002
2	-2.8388133825e-002	2	-1.8202980254e-002	2	-3.3492931571e-002
3	3.7501350060e-003	3	2.0749477038e-003	3	3.8025601997e-003
4	-1.8446699362e-004	4	-8.6995183107e-005	4	-1.6925890570e-004
5	3.1286830745e-006	5	1.2436524520e-006	5	2.6396519557e-006

radiometer 1		radiometer 2		radiometer 3	
H		H		H	
a 2i		a 2i		a 2i	
1	-1.2192070798e-002	1	-4.8938315835e-002	1	-5.1974877527e-003
2	8.8557322073e-003	2	2.6541378947e-002	2	1.0855313411e-002
3	-1.2734161054e-003	3	-3.7836135549e-003	3	-1.8411735248e-003
4	5.1704466145e-005	4	1.9204055354e-004	4	9.5714130699e-005
5	-5.8171521631e-007	5	-3.2620602022e-006	5	-1.6059448322e-006

Figure C1: The coefficients a $_{ki,p}$ in Eqn C2.

12 Appendix D: Variances for the Wind Retrieval

The variances needed in Eqn (2) - (3) are given in the table below.

wind speed	radiometer 1			radiometer 2			radiometer 3		
	sigma0_HH	TB H	W NCEP	sigma0_HH	TB H	W NCEP	sigma0_HH	TB H	W NCEP
0.0	0.002162	0.204694	1.118146	0.000478	0.196523	1.118146	0.000222	0.218601	1.118146
1.0	0.002811	0.216598	1.035427	0.000657	0.227773	1.035427	0.000253	0.244698	1.035427
2.0	0.003554	0.237533	0.941831	0.000837	0.260301	0.941831	0.000324	0.281098	0.941831
3.0	0.003397	0.244513	0.942946	0.000803	0.255531	0.942946	0.000319	0.281507	0.942946
4.0	0.003128	0.241825	0.961688	0.000755	0.244097	0.961688	0.000273	0.265312	0.961688
5.0	0.003005	0.237435	0.967645	0.000692	0.233588	0.967645	0.000257	0.253008	0.967645
6.0	0.002742	0.232175	0.965748	0.000605	0.223152	0.965748	0.000247	0.241897	0.965748
7.0	0.002561	0.232554	0.966377	0.000561	0.214750	0.966377	0.000251	0.232883	0.966377
8.0	0.002669	0.238376	0.982044	0.000589	0.214677	0.982044	0.000252	0.230973	0.982044
9.0	0.003058	0.243367	1.036862	0.000661	0.223211	1.036862	0.000284	0.241124	1.036862
10.0	0.003575	0.246757	1.121006	0.000768	0.235413	1.121006	0.000364	0.259865	1.121006
11.0	0.004267	0.264352	1.231900	0.000999	0.257846	1.231900	0.000474	0.286123	1.231900
12.0	0.005234	0.292643	1.344265	0.001326	0.291839	1.344265	0.000663	0.316673	1.344265
13.0	0.006088	0.316431	1.407236	0.001615	0.321048	1.407236	0.000803	0.339212	1.407236
14.0	0.006793	0.336506	1.427256	0.001938	0.336179	1.427256	0.000874	0.353528	1.427256
15.0	0.007678	0.361546	1.449059	0.002158	0.352008	1.449059	0.001027	0.377721	1.449059
16.0	0.008665	0.389540	1.527995	0.002431	0.393054	1.527995	0.001215	0.419884	1.527995
17.0	0.009586	0.416811	1.583605	0.002833	0.444346	1.583605	0.001321	0.467506	1.583605
18.0	0.010366	0.455024	1.643570	0.003222	0.483129	1.643570	0.001476	0.495254	1.643570
19.0	0.011534	0.489119	1.840392	0.003846	0.500000	1.840392	0.001586	0.500000	1.840392
20.0	0.012506	0.500000	2.073880	0.003906	0.500000	2.073880	0.001705	0.500000	2.073880
21.0	0.013046	0.500000	2.328262	0.003823	0.500000	2.328262	0.001769	0.500000	2.328262
22.0	0.013826	0.500000	2.637159	0.004314	0.500000	2.637159	0.001600	0.500000	2.637159
23.0	0.014606	0.500000	2.946057	0.004805	0.500000	2.946057	0.001431	0.500000	2.946057
24.0	0.015386	0.500000	3.254955	0.005297	0.500000	3.254955	0.001262	0.500000	3.254955
25.0	0.016166	0.500000	3.563852	0.005788	0.500000	3.563852	0.001094	0.500000	3.563852

13 Appendix E: Radiometer Calibration for V3.0

This appendix describes the status of the calibration of the radiometer in V3.0 of the Aquarius salinity retrieval and ground data processing.

The approach used to mitigate the radiometer drift has been modified. The drift is still divided into two parts, an exponential and wiggles (ATBD Addendum II). The exponential is treated as a gain

drift and the wiggles are treated as an offset (bias). Gain drift is corrected by adjusting the value of the reference noise diode, T_{ND}. The procedure is illustrated in Figure E1.

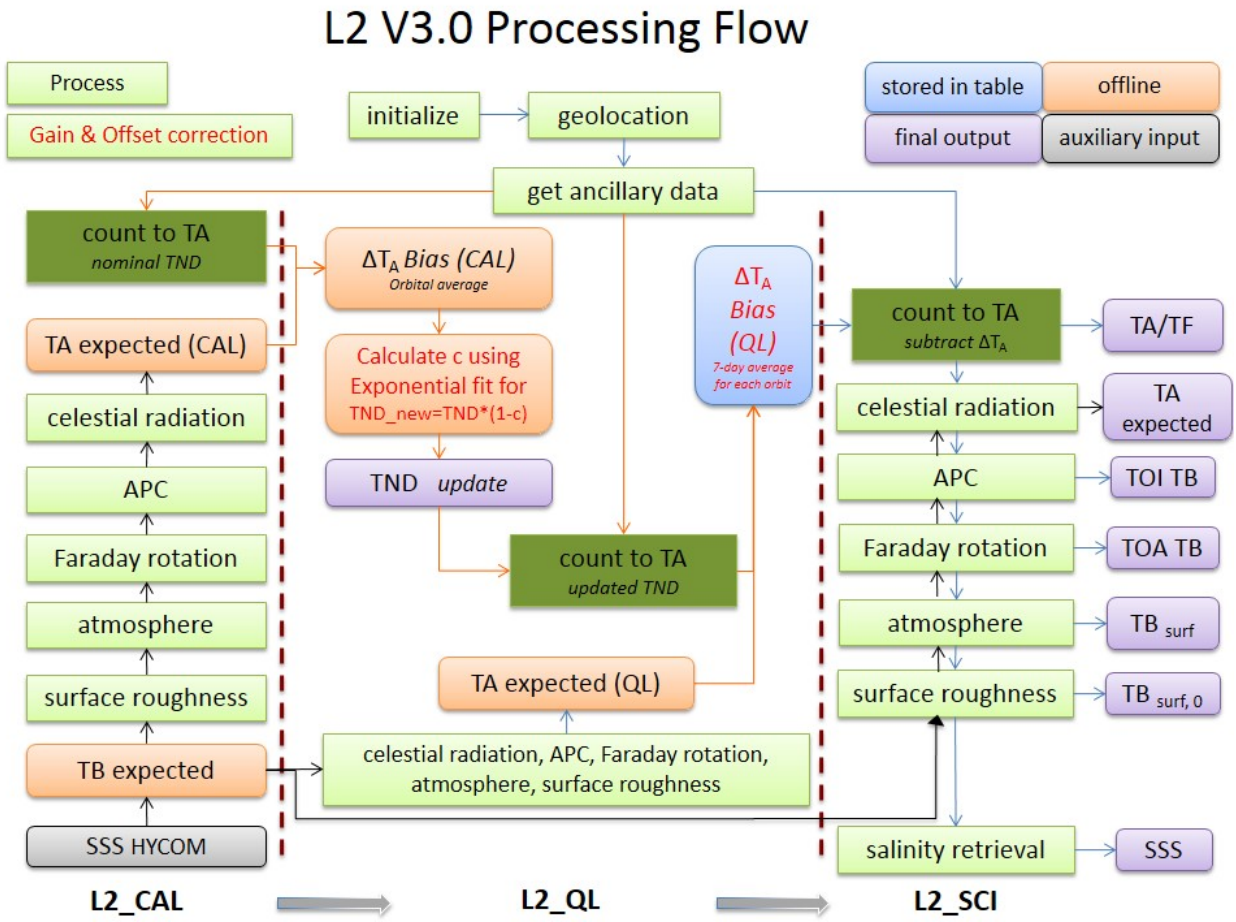

Figure E1: Schematic diagram of calibration drift correction. This diagram was provided by Liang Hong, GSFC.

E1: Calibration of the exponential drift (L2_CAL)

An exponential model is fitted to the radiometer gain drift. This is done once at the beginning of the version of the retrieval code (e.g. at the release of V3.0) and the fit remains fixed for that version. The process begins with the path labelled L2_CAL in Figure E1. The difference, TA – TA_expected, is computed for each orbit for all of the data since the beginning of the mission where TA is the radiometer output after the RFI filter (i.e. TF). The differences, labelled ΔT_A_bias(CAL) in the figure, are assumed to be due to a gain change and the change in the noise diode temperature, ΔT_{ND} corresponding for each difference is computed. The time series of ΔT_{ND} are then fitted to an exponential. The exponential remains unchanged for the lifetime of the version. During this computation:

a. The roughness correction is made using only the scatterometer sigma0 at HH polarization (i.e. the radiometer TB is not used).

b. The default value of $T_{ND,0}$ used to begin this computation is based on fitting TA to TA_expected during the first week of the mission. It is the same as the initial estimate of T_{ND} used in the conversion of counts to TA in V2.0 (Piepmeier et al, "Aquarius Radiometer Post Launch Calibration for Version 2, AQ-014-PS-0015). In effect the choice of $T_{ND,0}$ adjusts the radiometer output to conform to the global HYCOM salinity field during the first week.

The exponential computed above is used to correct the radiometer gain. This is done by adjusting the value of the T_{ND}. The process is outlined in Section L2_QL in Figure E1. The conversion from counts to TA is now repeated using a value of T_{ND} adjusted for the exponential drift. For each orbit the exponential is used to compute a new value of T_{ND} in the form:

$$T_{ND\,new} = T_{ND,0} \cdot (1 - c) \tag{E1}$$

where

$$c = A - B \cdot \exp(-D \cdot N) \tag{E2}$$

and N is the orbit number. The coefficients A, B and D are derived during the exponential fit described above; and the correction factor "c" is the adjustment predicted by the exponential change. The coefficient c is saved in the metadata of L2 files as "Delta TND H coefficient" and "Delta TND V coefficient" for each the 3 beams. The new value for TND is now used in the radiometer counts-to-TA conversion*. The orbit number, N, in Equation (E2) starts at launch (June 10) but Equation 2 is applied starting when Aquarius was turned on (August 25) which corresponds to N = 1150.

E2: Correction for the residual ("wiggles"): L2_QL

Then, a correction is made for the residual "wiggles" that remain after the exponential drift is removed. This is done by repeating step E.1 but with the up-dated TND (i.e. TND_new). TA_expected (same as in step E.1) is compared with the TA obtained using TND_new for the counts-to-TA calibration. The difference TA – TA_expected is called, ΔT_A_bias(QL). This is treated as a bias and removed from TA. "QL" in the figure means "Quick Look" to indicate the TA before a complete calibration has been performed.

a. This correction is applied to each orbit; however, the value used is a filtered (smoothed) estimate obtained using a window of 7 days.

b. This process is done once each month (i.e. the data is processed in batches of one-month).

This offset correction is saved in the metadata of L2 files as "Radiometer Offset Correction".

E.3. Data Used for Calibration

The data used in the processes outlined in steps E.1 and E.2 above used a subset of the L2 observations set aside for calibration. The flags and masks used to identify this subset are described in Table 1 of the "Aquarius Level-2 Data Product" specification document for V3.0 (AQ-014-PS-018) and in the "Proposal for Flags and Masks" for V3.0 (AQ-14-PS-0006).

E.4. Salinity Retrieval: L2_SCI

The measured TA calibrated using TND_new and with the bias ΔTA_bias(QL) removed is now used to retrieve salinity. The process (column L2_SCI in Figure E) is the inverse of the paths used to compute TA_expected in paths L2_CAL and L2_QL except that in the roughness correction the scatterometer and radiometer are used in the roughness correction (i.e. HH or HHH winds).

Note:

* TA used above is the radiometer output after correction for RFI. In the Aquarius documentation it is called "TF".